Data-driven accelerating the discovery of hole-doping induced 2D magnets

Junqiu An[a], Jiao Chen[a], Xiaotao Zhang[a], Hongyan Wang[a], Yongliang Tang[a], Yuxiang Ni[a], Yuan Ping Feng[b], Lei Shen[c, *], Haiyan Lu[d, *], Yuanzheng Chen[a, *]

[a] *School of Physical Science and Technology, Southwest Jiaotong University, Chengdu 610031, China*

[b] *Department of Physics and Centre for Advanced Two-Dimensional Materials, National University of Singapore, Singapore 117551, Singapore*

[c] *Department of Mechanical Engineering, National University of Singapore, Singapore 117575, Singapore*

[d] *Science and Technology on Surface Physics and Chemistry Laboratory, PO. Box 9-35, Jiangyou 621908, China*

* Corresponding authors.

E-mail addresses: cyz@swjtu.edu.cn (Y. Chen), shenlei@nus.edu.sg (L. Shen), hyluphys@163.com (H. Lu).

Keywords:

high-throughput screening; machine learning; hole-doping induced magnetism; 2D magnetic materials.

Abstract

Hole-doping induced 2D magnets (termed as HDIM), with hole-mediated magnetic state, not only fill in the scarce situation of 2D intrinsic magnets but also bring the great promise for next-generation spintronic nanodevices. However, current frameworks based on these first-principles calculations approaches for excavating HDIM show great blindness and laboriousness. Herein, a data-driven high-throughput screening framework was proposed to overcome this challenge. Utilizing and learning the data of Computational 2D Materials Database (C2DB), we identified the hole effective mass (HEM) as a physical descriptor for efficiently discovering HDIM, and developed an effective HEM machine learning model. Via the HEM-driven high-throughput screening framework, we screened the 2DMatPedia database and obtained a set of 477 high-stability HDIM candidates. Combination with high-throughput calculations assess that up to 35 % exhibit significant HDIM-associated properties. For example, finding a novel HDIM of $ZrMo_2O_8$, with a fantastic honeycomb-checkerboard 2D architecture, demonstrates hole-doped induced rarely half-metallic ferromagnetism and high Curie temperature. This proposed data-driven framework offers a high-efficiency approach toward accelerating the discovery of 2D tunable magnets.

1. Introduction

Two-dimensional (2D) magnets,[1-3] possessing atomic-scale magnetic characteristics, offer an ideal nanomaterial platform and magnetism source for spintronic nanodevices (i.e., spin field effect transistors,[4] spin tunnel junctions,[5] spin light-emitting diodes[6]), which arouse substantial research interest of scientists. According to the Mermin-Wagner theorem,[7] the long-range magnetic order in 2D Heisenberg spin systems is theoretically impossible at a limited temperature, thus consequently it is not easy to achieve 2D intrinsic magnets. In the past decade, although many efforts had been devoted to theoretically or experimentally exploring 2D intrinsic magnets, it is depressing that successful cases are very scarce and only a few such as CrI_3, Fe_3GeTe_2, $Cr_2Ge_2Te_6$, VSe_2, etc. are reported so far.[8-12]

To avoid the bottleneck of 2D intrinsic magnets, one notable idea is that by an induced strategy (i.e., defect,[14-16] strain,[17] adsorption,[18-19] chemical functionalization,[20-21] hole doping[22-25]) introduce magnetism into 2D nonmagnetic systems. Among these strategies ongoing research on inducing 2D magnets, hole doping can control the carrier concentration of magnets by electrical

means (i.e., gate bias, electrolyte gating), which more easily integrates in devices and does not change material composition. Meanwhile, due to the atomic-level thickness of 2D materials, adopting the electrolyte gating technology can adjust the hole doping concentration to the order of $10^{13} \sim 10^{14}$ cm^{-2}.[26-27] At present, several 2D systems (i.e., GaSe, α-SnO, KTLO) [28-30] have demonstrated that a spontaneous ferromagnetic transition can occur in such hole-doping concentration. Therefore, searching for hole-doping induced 2D magnets (HDIM) is of great potential value in spintronic applications.

Currently, the approach for screening whether 2D nonmagnetic systems can be transform into HDIM candidate just depend on the first-principles calculations,[28-30], and the seeking direction is usually random, these factor leading the obtained HDIM cases are very rare. Recently, high-throughput screening[31-35] has been proved to be an effective strategy for discovering new 2D magnets through from 2D material databases. Very recent, an exciting work was made by Michel *et al*[36] who combined first-principles calculations with high-throughput screening and identified 122 HDIM from a 2D materials database of C2DB.[31] But, in this work their brute-force calculations scheme is very laborious, cumbersome, and time-consuming, which make such scheme cannot apply for the big database. It is thus highly desirable to a high-efficiency screening framework that can serve to any 2D database resources on exploring HDIM.

This desired framework is very challenging, which should solve two key problems: (i) finding effective HDIM descriptor to accurately screen candidates in order to avoid one-by-one blind calculation; (ii) realizing the prediction of HDIM descriptor to avoid that some databases cannot directly offer the descriptor data. Under these problems driven, we adopt machine learning (ML) technology[37-40] combined with high-throughput screening approach to develop a data-driven high-throughput screening framework for overcoming the above challenge. Utilizing the data of C2DB, we identified the hole effective mass (HEM) as a descriptor to characterize the van Hove singularity near the Fermi level, inducing and tuning the magnetism in hole-doped 2D materials. To address the lack of HEM-data for 2D materials, we further developed a machine learning model to predict HEM for 2D materials. Based on the HEM-driven high-throughput screening framework, we screened the new 2D material database (2DMatPedia)[41] and obtained a set of 477 high-stability HDIM candidates. Combination with high-throughput calculations assess that up to 35 % exhibit

significant HDIM-associated properties. This work introduces a novel strategy that combines a descriptor-based approach, machine learning, and high-throughput screening to accelerate the discovery of new HDIM, substantially enriching the family of 2D tunable magnets.

2. Computational Methods

Within the framework of spin-polarized density functional theory (DFT), our first-principles calculations were performed using a projector-augmented wave (PAW) method[42] as implemented in the Vienna *ab initio* simulation package (VASP).[43] The generalized gradient approximation with Perdew−Burke−Ernzerhof parametrization (GGA-PBE)[44] was applied as the exchange−correlation functional, and the density functional dispersion correction (D3-Grimme)[45] was adopted for a better description of the van der Waals interactions between layers. A cutoff energy of 600 eV was set for the plane wave basis. The convergence criteria were 1×10^{-2} eV/Å for the residual forces on ions and 1×10^{-6} eV for the energy difference in electronic self-consistent loop. The Brillouin zone sampling is performed with a Monkhorst–Pack k-point mesh[46] of a density of $2\pi \times 0.04$ Å^{-1} to keep the energy convergence. In the carrier doping calculations, the carrier density was tuned by changing the number of electrons from the cell, with a jellium background with opposite charge added to maintain charge neutrality and the crystal structures are reoptimized at different carrier densities. The spin polarization energies for various systems with hole doping have been obtained using this approach.

3. Results and Discussion

3.1. Descriptor

According to the Stoner criterion,[23, 47-48] large density of states (DOS) near the Fermi level is generally an indication of electronic instabilities and transitions to different phases, such as magnetism. Therefore, tunable magnetism of materials can be judged intuitively according to the van Hove singularity (VHs) near the Fermi level. However, VHs is a qualitative concept used to represent high DOS, which cannot be directly used in high-throughput screening as a searching condition because it is not a quantitative physical quantity. To find suitable and quantitative descriptors for tunable magnetic materials, we carry out the data analysis on some reported tunable magnetic materials (i.e., GaSe, InP_3) as listed in **Table S1** and **Fig. S1**. Their common features

are semiconductors with relatively high HEM (the HEM value is usual greater than 1 m_0). In addition, note that some intrinsic ferromagnetic semiconductors also have heavy HEM and exhibit similar band structure near the Fermi level, such as h-CrC[49], NbS_2[50].

In fact, the effective mass is closely related to the electronic band structure of materials. For a material with VHs near VBM, there is a high DOS (or flat band) near VBM, leading to a large HEM because the second derivative of the band curve is inversely proportional to the HEM. Therefore, a high HEM is an important feature of materials with VHs near VBM, and thus can be used as an important screening descriptor for 2D tunable magnetic materials.

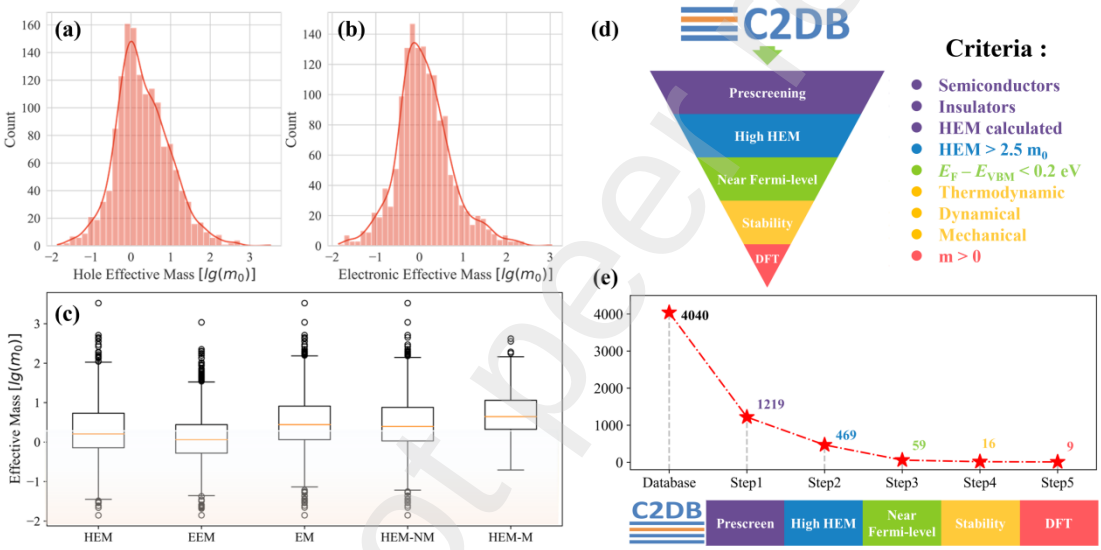

Fig. 1. Histograms of (a) hole effective mass and (b) electronic effective mass distribution in C2DB. (c) Boxplot of hole effective mass (HEM), electronic effective mass (EEM), effective mass maximum (EM), the HEM of non-magnetic (HEM-NM), and the HEM of magnetic materials (HEM-M) from left to right. The orange horizontal line represents the median value. Outliners are marked with hollow dots. (d-e) The workflow of the high-throughput screening scheme applied on C2DB to identify potential 2D materials with hole-doping induced and/or controlled magnetism.

The above understanding qualitatively provides a physically meaningful descriptor for searching the host candidates which can be potentially induced into magnets by hole doping or tunable magnets by varying the hole concentration. The next step is to quantitively determine the proper threshold of the hole effective mass. To obtain a data-driven distribution of effective mass of 2D materials, we take the C2DB database which

directly offers the data of band gap, band edges, and effective mass over 4000 2D materials. It is worth noting that we merely take into account the maximum of effective mass in various directions. The histograms in **Fig. 1a** and **1b** show the distributions of HEM and EEM, respectively. With standard deviations of 0.69 and 0.63 lg(m_0) and mean values of 0.30 and 0.11 lg(m_0) for the two histograms, respectively, they are approximately in normal distribution. As shown in **Fig. 1c**, the effective mass maximum of magnetic materials is higher than that of non-magnetic materials overall. The obvious difference between the effective mass of magnetic and non-magnetic materials also implies that the effective mass can be used as one of the screening conditions for tunable magnetic materials. Thus, high effective mass can be used to characterize the VHs near the Fermi-level, which are adopted to apply in the high-throughput screening of tunable magnetic materials as follows. According to the data analysis from C2DB, the HEM median value of non-magnetic materials is greater or equal to 2.5 m_0, which can be an appropriate threshold for high-throughput screening.

3.2. High-Throughput Screening Process

Fig. 1d and **1e** show the detailed workflow of our high-throughput screening process of 2D tunable magnets. We use 4040 2D materials from C2DB as the input data. To narrow down our search range, we perform preliminary screening criterion for the high-throughput screening. Target materials must be semiconductors or insulators with calculated effective mass. In this step, database tool in ASE[51] package is used to obtain materials properties including effective mass data automatically, narrowing down to 1454 material candidates. For the effective mass of nonmagnetic materials, the screening threshold of HEM is set at the median value ($>$ 2.5 m_0) and 26 outliers are removed to ensure HEM within this range. For the remaining 1428 materials, we focus on only non-magnetic materials and obtain 1219 materials for further screening.

After preliminary screening, we then analyze whether a material shows the VHs near the Fermi-level in its electronic band structure. In this stage, 469 over 1219 materials are considered as candidates with higher DOS, and 59 materials with $E_F - E_{VBM} < 0.2$ eV are further obtained, where E_F is the Fermi energy and E_{VBM} is the energy of valence band maximum. The low energy difference of 0.2 eV is to promise the VHs close to the Fermi-level. Finally, according to the thermal and dynamical stability criterion, we got 16 2D material candidates with high-stability and high potential to be HDIM materials as listed in **Table S2**.

To verify whether our screened results have hole-doping induced magnetism, a

variety of low hole-doping concentrations (0.2 - 0.6 hole/f.u.) and DFT calculations are conducted. After full optimization of the doped cells, we calculated the magnetic moment and the magnetic energy, which is defined as the total energy difference between the nonmagnetic and ferromagnetic states ($E_{Mag} = E_{NM} - E_{FM}$). The magnetic moments of screened results with different hole-doping concentrations are listed in **Table S3**. Among the 16 materials selected, nine candidates ($Co_2H_2S_4$, Tl_2Te_2, $Co_2Cl_2S_2$, $Co_2H_2O_4$, $Rh_2Ta_2Te_8$, $Co_4Br_4O_4$, Nb_4S_{12}, V_4O_8 and Cu_2O_2) show magnetism at a certain concentration of hole doping **(Table 1)**. Note that these candidate materials have not been reported in the previous works. In contrast to previous brute-force high-throughput DFT calculations for identifying potential 2D magnetic materials induced by hole doping,[36] our rational scheme utilizes the high HEM as a key descriptor of searching criteria combining with high-throughput screening, which can achieve high accuracy at low computational cost. The HEM screening threshold we set is slightly higher, and more accurate candidates could be yielded.

Table 1. Nine 2D tunable magnetism candidates validated by DFT calculation from high-throughput screening results.

Formula	Space group	Bandgap [eV]	HEM [m_0]	EEM [m_0]
$Co_2H_2S_4$	*P*2_1/*m*	0.36	10.66	7.37
Tl_2Te_2	*P*-3*m*1	0.29	10.31	0.08
$Co_2Cl_2S_2$	*Pmmn*	0.01	7.73	1.21
$Co_2H_2O_4$	*P*2_1/*m*	0.39	5.14	6.64
$Rh_2Ta_2Te_8$	*P*2_1/*m*	0.08	3.47	5.97
$Co_4Br_4O_4$	*P*2_1/*c*	0.18	5.87	1.85
Nb_4S_{12}	*P*2_1/*m*	0.38	4.64	0.59
V_4O_8	*C*2/*m*	0.31	3.61	2.76
Cu_2O_2	*P*2/*m*	0.01	2.97	1.35

3.3. DFT Verification

To confirm the validity of the above high-throughput screening, we select three candidates ($Co_4Br_4O_4$, Nb_4S_{12} and V_4O_8) that they can arrive at 1.0 μB/carrier, and calculate their electron spin magnetic moments at a wide hole doping level (0 - 2.0 hole/f.u.) **(Fig. 2)**. All their DOS and band structures **(Fig. S2)** have an obvious VHs at or near E_F and all have a Stoner-type magnetic instability with hole doping, leading to

a metallic ferromagnetic or antiferromagnetic state. The calculations show that the hole-doping $Co_4Br_4O_4$ or Nb_4S_{12} spontaneously evolves into a ferromagnetic ground state even at a small amount (~0.2 hole/f.u.) of hole doping (**Table S4** and **S5**). While the ΔE_{FM-AFM} of hole-doped V_4O_8, which is the total energy difference between the ferromagnetic-polarized and anti-ferromagnetic-polarized states, is calculated to confirm its stability of anti-ferromagnetic state **(Table S6)**. At a high hole-doping density of ~ 0.5 hole/f.u., the curves of their magnetic moments show a link, and all can arrive at a large value of 1.0 μ_B/carrier, indicating the injected holes induced a fully spin polarized. The physical origin of magnetism upon hole doping for these 2D systems can be understood by considering the Stoner mechanism, which is strongly correlated with the physical descriptor of HEM and VHs near E_F. To understand this behavior, we investigate the electronic structure of these three candidates, and notice that their magnetic moments are contributed mainly by the states at the top of the valence band, which has mostly anion p character. In the band-picture model, spontaneous ferromagnetism occurs when the relative gain in exchange interaction is larger than the loss in kinetic energy, i.e., when it satisfies the ''Stoner Criterion'': $\mathrm{D}(E_f)J > 1$, where $\mathrm{D}(E_f)$ is the DOS at the Fermi energy, and J denotes the strength of the exchange interaction[52]. As shown in **Fig. S2** and **Table S4-S6**, our calculated results can easily be explained by this model. In a short summary, the reasons that these candidates can be spin-polarized by injecting holes are as follows: (i) the p states contribute a very large exchange interaction J; (ii) the valence band maximum is quite flat with large HEM (m_0). Because the density of states $\mathrm{D}(E_f)$ is proportional to $m_0{}^{3/2}\sqrt{E_{VBM} - E_f}$ when holes are introduced, magnetization can be sustained in these large HEM candidates.

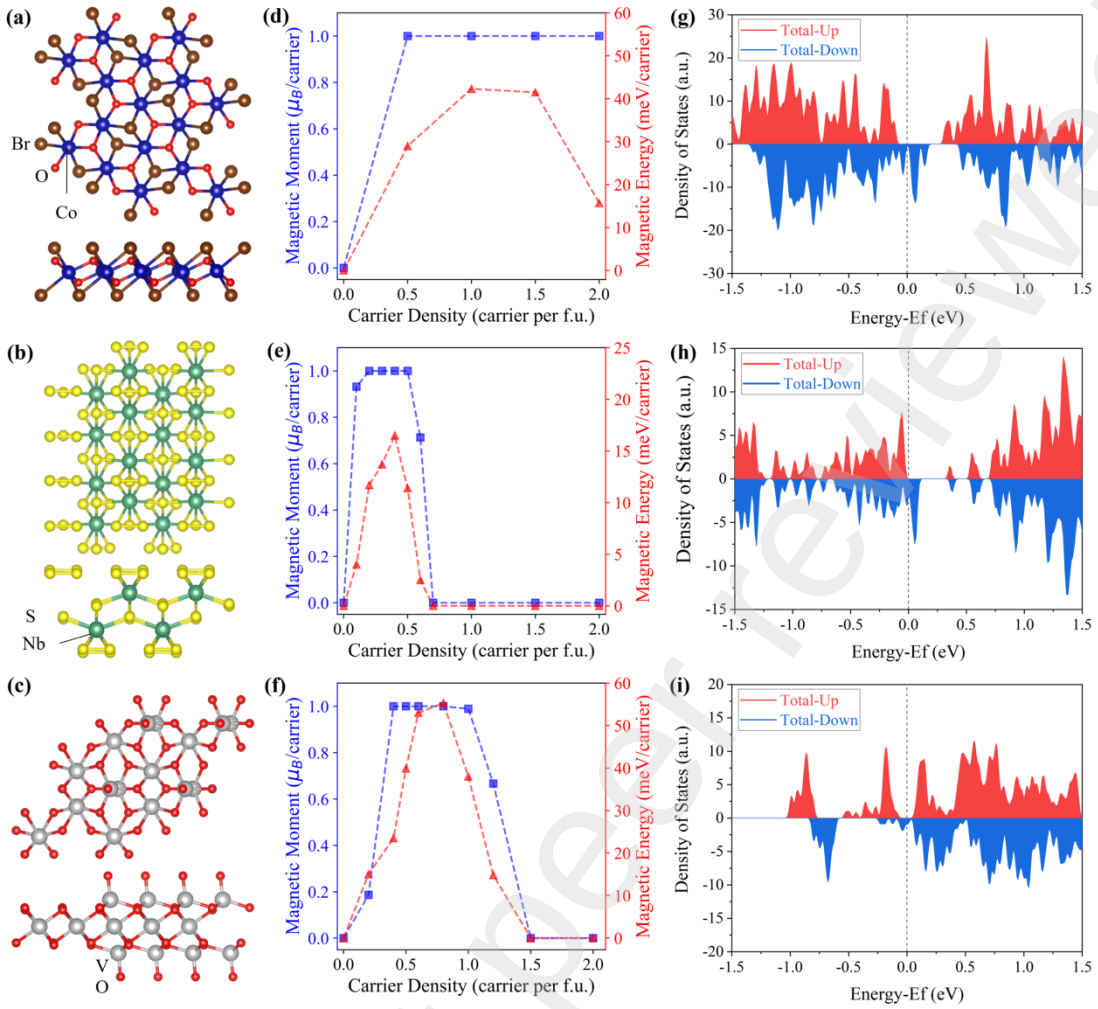

Fig. 2. Geometry structures of (a) $Co_4Br_4O_4$, (b) Nb_4S_{12} and (c) V_4O_8 monolayers with top and side views, respectively. Calculated magnetic moment and magnetic energy of (d) $Co_4Br_4O_4$, (e) Nb_4S_{12} and (f) V_4O_8 monolayers as a function of carrier density, respectively. Density of states of (g) $Co_4Br_4O_4$ monolayer at a carrier density of 3×10^{14} cm^{-2}, (h) Nb_4S_{12} monolayer at a carrier density of 7.3×10^{13} cm^{-2} and (i) V_4O_8 monolayer at a carrier density of 3×10^{14} cm^{-2}, respectively. At these concentrations, the magnetic energies of the materials reach their peak values. The dashed line at 0 eV indicates the Fermi energy.

3.4. ML Effective Mass Prediction

At present, a large number of new 2D materials have been reported or synthesized, for example, the latest 2D database "2DMatPedia" provides more than 10,000 2D materials, but it does not provide HEM data. Thus, one cannot directly obtain the HEM descriptor to screen the HDIM materials in 2DMatPedia. Based on the 1454 datasets from the C2DB database, we develop an end-to-end machine learning model to predict

the effective mass of 2D materials, which can be used as a descriptor for quickly pre-screening 2D materials that potentially possesses HEM tunable magnetism. In our work, materials with HEM < m_0 are labeled as "0", indicating that their hole effective mass is low, and they may have a higher carrier mobility, while materials with HEM > 1 m_0 are labeled as "1", indicating that they are more likely to be magnets after hole doping.

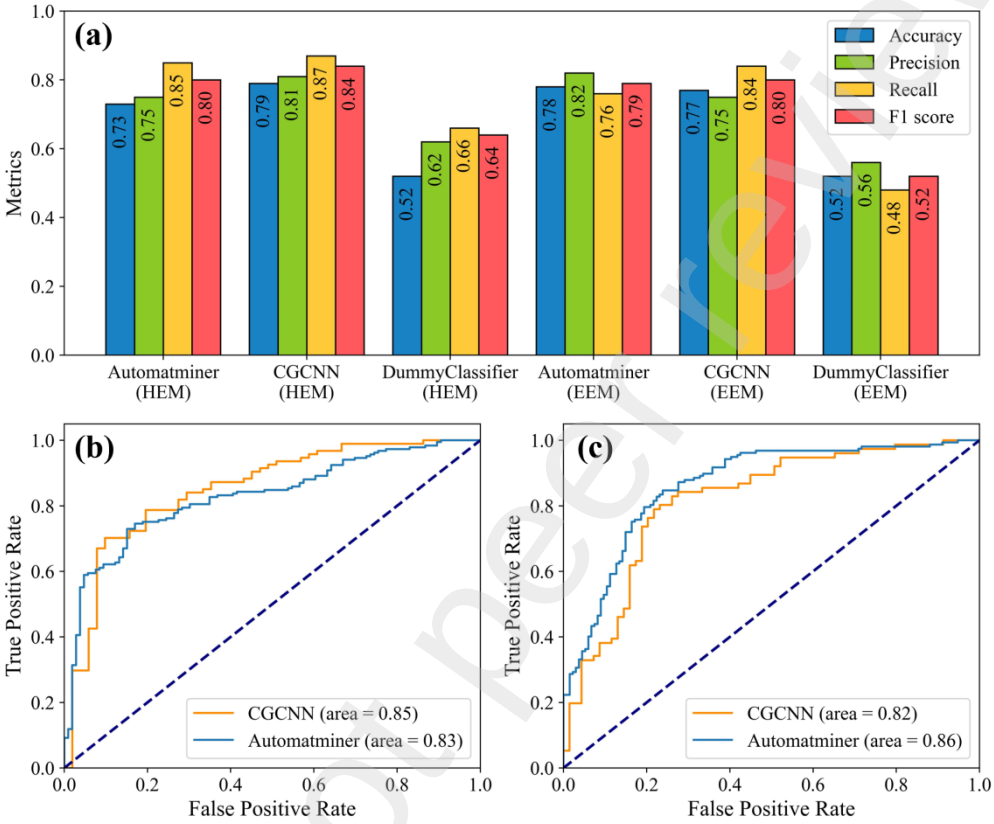

Fig. 3. (a) Metrics of various machine learning classification models on testing set. Receiver Operating Characteristic curve visualizing the result of (b) HEM and (c) EEM classification, respectively. It plots the proportion of correctly identified class '1' (true positive rate) against the proportion of wrongly identified class '0' (false positive rate) under different thresholds.

In order to obtain accurate ML models, we compared deep learning models represented by Crystal Graph Convolutional Neural Networks (CGCNN)[53] with automatminer machine learning models[54]. As shown in **Fig. 3a** and **Table S7**, both these two models for predicting HEM are higher than the baseline model based on distribution strategy constructed using the scikit-learn framework, DummyClassifier. Especially, their accuracy and precision are about 0.7 ~ 0.8, while Recall, F1 score, and AUC are higher than 0.8. Similarly, using the same approach, we also constructed

machine learning models for predicting electronic effective mass (EEM). The evaluating metrics of EEM and HEM predictions are numerical close. Besides, the similarity of their ROC curves **(Fig. 3b and 3c)** also indicates that the performances of these two ML methods are notable similar for the task of predicting HEM and EEM.

3.5. ML Application on New Database

To expedite the discovery of novel 2D tunable magnetic materials, we applied the CGCNN and automatminer ML models described above to another larger 2D material database (2DMatPedia), which lacks effective mass information, for predicting the hole effective mass of all non-magnetic semiconducting materials in 2DMatPedia **(Fig. 4)**. 2045 materials are identified that their HEM is to belong to category "1" by both these two models. From the high-HEM materials, we selected the low energy difference between the Fermi level and the VBM ($E_F - E_{VBM} < 0.2$ eV) to obtain 1084 potential 2D materials with the VHs near E_F. Afterwards, we verify the stability of the potential candidates with respect to the cohesive energy $E_c > 200$ meV/atom and the exfoliation energy $E_{exf} < 100$ meV/atom, we obtain 477 candidates with high thermodynamic stability **(Table S8)**. As a result, these 477 materials can be recognized as potential stable tunable magnetic materials with hole-doping.

To verify the potential candidates mentioned above, we evaluate their magnetic behaviors at different hole-doping concentrations using high-throughput DFT calculations. It is worth noting that we only select 100 materials randomly from the 477 candidates due to the significant computational cost associated with varying the doping concentration across approximately 500 hosts. It is found that a high 35 percent (seeing the validated 35 HDIM materials in **Table S9**) are identified to exhibit hole-doping induced magnetism. Thus, this approach combined pre-screening and ML model shows its efficiency to narrow down the potential candidates from a huge search space. In comparison, we randomly select 100 materials from the total 10000 materials in 2DMatPedia database, and do not obtain any HDIM candidates finally. This fact verifies our HEM data-driven method combining advanced ML techniques with high-throughput screening can be powerful to form an effective framework for the acceleration of the discovery of 2D tunable magnetic materials. Moreover, this data-driven method can be developed to form an adaptive EEM framework for exploring electron-doping induced tunable magnetic materials in future.

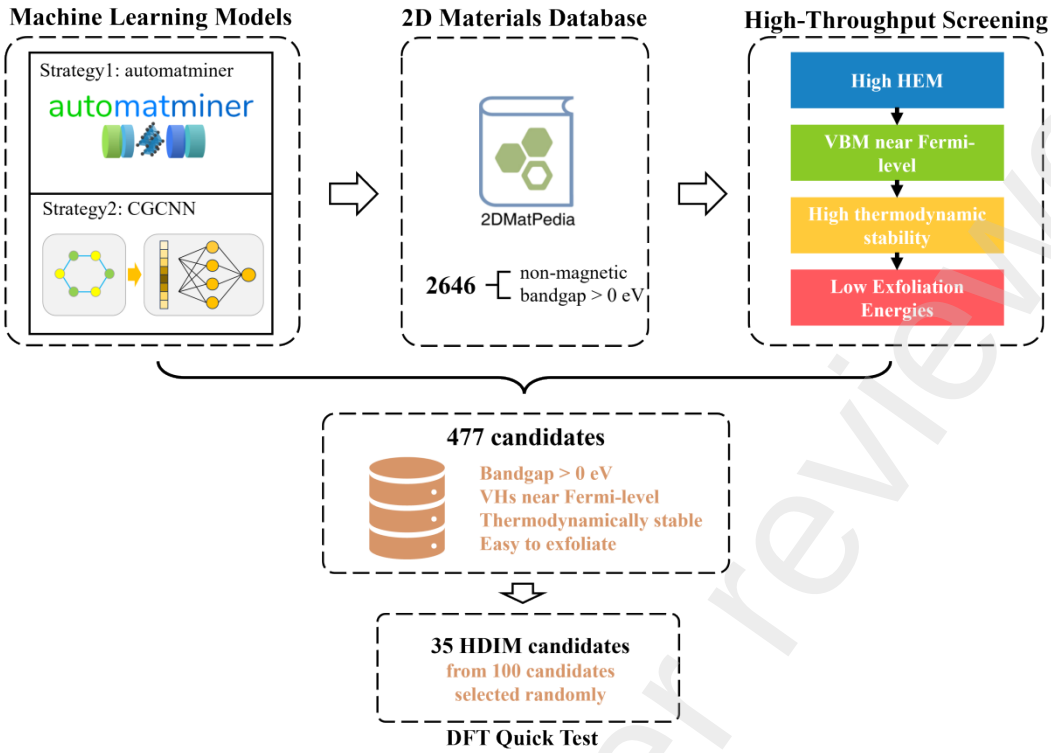

Fig. 4. The workflow of high-throughput screening applied to 2DMatPedia for identifying potential 2D tunable magnetic materials.

3.6. A Case of $ZrMo_2O_8$

From above 35 candidates, a transition bimetallic oxide monolayer, $ZrMo_2O_8$ **(Fig. 5a-5b)**, has a unique atomic feature and magnetic behavior, in which each Zr (Mo) atom bonds to six (four) neighboring O atoms and form two nested dodecagonal and octagonal frameworks. This transition metal oxide monolayer shows remarkable honeycomb-checkboard pattern, which is different from the traditional structure of 2D magnetic materials, such as CrI_3. Additionally, the hole-doped $ZrMo_2O_8$ monolayer becomes half-metallic **(Fig. 5c-5d)** with a magnetic moment of 1 μB/carrier and a large magnetic energy of 10 meV/carrier at a carrier density of 1.54×10^{14} cm^{-2} (0.5 hole/f.u.).

In order to understand the underlying physics of such unique atomic structure and magnetic properties, we perform an orbital projected density of states (PDOS) analysis. It is found that the magnetic moments in hole-doped $ZrMo_2O_8$ monolayer are mainly dominated by the 2*p* orbital of O atoms and the spin-density is primarily from the O atoms along the out-of-plane direction as illustrated in **Fig. 5b**. Its Curie temperature T_c is computed to be 126 K under the hole doping density of 1.54×10^{14} cm^{-2}, and further increases to 243 K at increasing the hole doping density of 3×10^{14} cm^{-2} **(Fig. 5e)**. **Fig. S6** reveals the magnetic coupling mechanism, in which the direct out-of-plane magnetic

interaction mainly arises from the exchange coupling between the O p_z orbital. Moreover, a non-negligible hybridization between the O p_x/p_y orbitals (spin-down) and the Mo p_x/p_y or d_{xz}/d_{yz} orbitals (spin-down) near the Fermi level indicates the indirect exchange interaction, involving the coupling between the O p_x/p_y orbitals with the Mo p orbitals. This indirect exchange coupling also plays an important role in the ferromagnetic exchange mechanisms. This novel material not only enriches the family of 2D tunable magnetic materials, but also provides a unique magnetic coupling mechanism in 2D magnetic materials. These findings of such HDIM suggest that they will expand the magnetic functionality and find valuable applications in electrically tuning spintronic nanodevices.

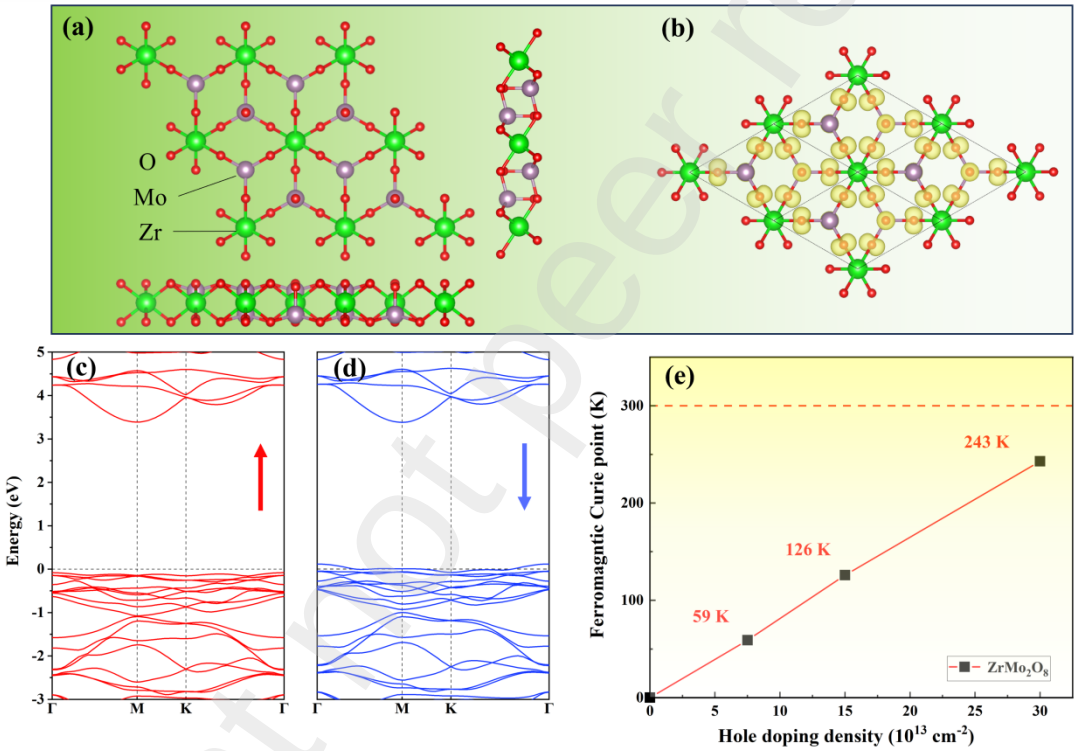

Fig. 5. (a) Geometry structures of $ZrMo_2O_8$ monolayer with top and side views, respectively. (b) Electronic band structure of 2D $ZrMo_2O_8$ at a carrier density of 0.5 hole/f.u. The dashed line at 0 eV indicates the Fermi energy. The red and blue curves represent spin-up and spin-down, respectively. (c) The spin charge density distribution of 2D $ZrMo_2O_8$. (d) The hole-doping concentration-dependent FM Curie temperatures in $ZrMo_2O_8$ monolayer.

4. Conclusions

In this work, we identify a data-driven effective descriptor for accelerating the

discovery of 2D magnetic materials with tunable magnetic behavior. Utilizing the HEM descriptor and high-throughput first-principles calculations, we successfully discover nine novel HDIM materials (i.e., $Co_2H_2S_4$, Tl_2Te_2, $Co_2Cl_2S_2$, $Co_2H_2O_4$) from the C2DB database. Furthermore, we develop machine learning models for predicting HEM of 2646 2D materials in the 2DMatPedia database which lacks effective mass information. Combined with high-throughput screening, we outline 477 high-stability 2D material hosts that could potentially become 2D magnets by hole-doping. Among them, approximately 35 percent of the candidates are identified to exhibit hole-doping induced magnetism by DFT evaluations. Interestingly, we discover a remarkable honeycomb-checkboard pattern candidate, $ZrMo_2O_8$, with hole-doping half-metallic ferromagnetism and high Curie temperature. The strategy of data-driven descriptors together with high-throughput calculations holds the promising for quickly uncovering many new 2D magnets.

CRediT authorship contribution statement

Junqiu An (Data curation: Lead; Investigation: Lead; Methodology: Lead; Writing – original draft: Lead)

Jiao Chen (Formal analysis: Equal; Investigation: Supporting; Methodology: Supporting)

Xiaotao Zhang (Data curation: Supporting; Investigation: Supporting; Methodology: Supporting)

Hongyan Wang (Formal analysis: Supporting; Resources: Supporting; Validation: Supporting)

Yongliang Tang (Formal analysis: Supporting; Resources: Supporting; Validation: Supporting)

Yuxiang Ni (Formal analysis: Supporting; Resources: Supporting; Validation: Supporting)

Yuan Ping Feng (Resources: Supporting; Software: Supporting; Visualization: Supporting)

Lei Shen (Conceptualization: Supporting; Supervision: Supporting; Writing – review & editing: Supporting)

Haiyan Lu (Conceptualization: Supporting; Supervision: Supporting; Writing – review & editing: Supporting)

Yuanzheng Chen (Conceptualization: Lead; Supervision: Lead; Writing – review &

editing: Lead)

Declaration of Competing Interest

The authors declare that they have no known competing financial interests or personal relationships that could have appeared to influence the work reported in this paper.

Data Availability

The data that support the findings of this study are available from the corresponding author upon reasonable request.

Acknowledgements

This work was supported by the National Natural Science Foundation of China (12164009), the Sichuan Science and Technology program (2022ZYD0024), and Singapore MOE Tier 1 (No. A-8001194-00-00) and Singapore MOE Tier 2 (No. A-8001872-00-00).

Appendix A. Supporting information

Supplementary data associated with this article can be found in the online version.

References

[1] K.S. Novoselov, A.K. Geim, S.V. Morozov, D. Jiang, Y. Zhang, S.V. Dubonos, I.V. Grigorieva, A.A. Firsov, Electric field effect in atomically thin carbon films, Science 306 (2004) 666-669, https://doi.org/10.1126/science.1102896.

[2] K.S. Novoselov, A.K. Geim, S.V. Morozov, D. Jiang, M.I. Katsnelson, I.V. Grigorieva, S.V. Dubonos, A.A. Firsov, Two-dimensional gas of massless Dirac fermions in graphene, Nature 438 (2005) 197-200, https://doi.org/10.1038/nature04233.

[3] Y. Hernandez, V. Nicolosi, M. Lotya, F.M. Blighe, Z.Y. Sun, S. De, I.T. McGovern, B. Holland, M. Byrne, Y.K. Gun'ko, J.J. Boland, P. Niraj, G. Duesberg, S. Krishnamurthy, R. Goodhue, J. Hutchison, V. Scardaci, A.C. Ferrari, J.N. Coleman, High-yield production of graphene by liquid-phase exfoliation of graphite, Nat. Nanotechnol. 3 (2008) 563-568, https://doi.org/10.1038/nnano.2008.215.

[4] Y.P. Feng, L. Shen, M. Yang, A. Wang, M. Zeng, Q. Wu, S. Chintalapati, C.R. Chang, Prospects of spintronics based on 2D materials, WIREs Comput. Mol. Sci. 7 (2017) e1313, https://doi.org/10.1002/wcms.1313.

[5] L. Zhang, J. Zhou, H. Li, L. Shen, Y.P. Feng, Recent progress and challenges in magnetic tunnel junctions with 2D materials for spintronic applications, Appl. Phys. Rev. 8 (2021) 021308, https://doi.org/10.1063/5.0032538.

[6] E. Elahi, G. Dastgeer, G. Nazir, S. Nisar, M. Bashir, H. Akhter Qureshi, D.-k. Kim, J. Aziz, M. Aslam,

K. Hussain, M.A. Assiri, M. Imran, A review on two-dimensional (2D) magnetic materials and their potential applications in spintronics and spin-caloritronic, Comp. Mater. Sci. 213 (2022) 111670, https://doi.org/10.1016/j.commatsci.2022.111670.

[7] N.D. Mermin, H. Wagner, Absence of ferromagnetism or antiferromagnetism in one- or two-dimensional isotropic heisenberg models, Phys. Rev. Lett. 17 (1966) 1133-1136, https://doi.org/10.1103/PhysRevLett.17.1133.

[8] B. Huang, G. Clark, E. Navarro-Moratalla, D.R. Klein, R. Cheng, K.L. Seyler, D. Zhong, E. Schmidgall, M.A. McGuire, D.H. Cobden, W. Yao, D. Xiao, P. Jarillo-Herrero, X. Xu, Layer-dependent ferromagnetism in a van der Waals crystal down to the monolayer limit, Nature 546 (2017) 270-273, https://doi.org/10.1038/nature22391.

[9] H.H. Kim, B. Yang, S. Li, S. Jiang, C. Jin, Z. Tao, G. Nichols, F. Sfigakis, S. Zhong, C. Li, S. Tian, D.G. Cory, G.X. Miao, J. Shan, K.F. Mak, H. Lei, K. Sun, L. Zhao, A.W. Tsen, Evolution of interlayer and intralayer magnetism in three atomically thin chromium trihalides, Proc. Natl. Acad. Sci. U.S.A. 116 (2019) 11131-11136, https://doi.org/10.1073/pnas.1902100116.

[10] L. Pan, H. Wen, L. Huang, L. Chen, H.-X. Deng, J.-B. Xia, Z. Wei, Two-dimensional XSe_2 (X= Mn, V) based magnetic tunneling junctions with high Curie temperature, Chinese Phys. B 28 (2019) 107504, https://doi.org/10.1088/1674-1056/ab3e45.

[11] X. Zhang, B. Wang, Y. Guo, Y. Zhang, Y. Chen, J. Wang, High Curie temperature and intrinsic ferromagnetic half-metallicity in two-dimensional Cr_3X_4 (X = S, Se, Te) nanosheets, Nanoscale Horiz. 4 (2019) 859-866, https://doi.org/10.1039/C9NH00038K.

[12] L. Zhang, L. Song, H. Dai, J.-H. Yuan, M. Wang, X. Huang, L. Qiao, H. Cheng, X. Wang, W. Ren, X. Miao, L. Ye, K.-H. Xue, J.-B. Han, Substrate-modulated ferromagnetism of two-dimensional Fe3GeTe2, Appl. Phys. Lett. 116 (2020) 042402, https://doi.org/10.1063/1.5142077.

[13] X. Jiang, Q. Liu, J. Xing, N. Liu, Y. Guo, Z. Liu, J. Zhao, Recent progress on 2D magnets: Fundamental mechanism, structural design and modification, Appl. Phys. Rev. 8 (2021) 031305, https://doi.org/10.1063/5.0039979.

[14] K. Pi, K.M. McCreary, W. Bao, W. Han, Y.F. Chiang, Y. Li, S.W. Tsai, C.N. Lau, R.K. Kawakami, Electronic doping and scattering by transition metals on graphene, Phys. Rev. B 80 (2009) 075406, https://doi.org/10.1103/PhysRevB.80.075406.

[15] B. Huang, H.J. Xiang, J.J. Yu, S.H. Wei, Effective control of the charge and magnetic states of transition-metal atoms on single-layer boron nitride, Phys. Rev. Lett. 108 (2012) 206802, https://doi.org/10.1103/PhysRevLett.108.206802.

[16] A. Ramasubramaniam, D. Naveh, One-dimensional half-metallic interfaces of two-dimensional honeycomb insulators, Phys. Rev. B 87 (2013) 161411, https://doi.org/10.1103/PhysRevB.88.161411.

[17] W.S. Yun, J.D. Lee, Strain-induced magnetism in single-layer MoS_2: origin and manipulation, J. Phys. Chem. C 119 (2015) 2822-2827, https://doi.org/10.1021/jp510308a.

[18] H. Gonzalez-Herrero, J.M. Gomez-Rodriguez, P. Mallet, M. Moaied, J.J. Palacios, C. Salgado, M.M. Ugeda, J.Y. Veuillen, F. Yndurain, I. Brihuega, Atomic-scale control of graphene magnetism by using hydrogen atoms, Science 352 (2016) 437-441, https://doi.org/10.1126/science.aad8038.

[19] P. Manchanda, A. Enders, D.J. Sellmyer, R. Skomski, Hydrogen-induced ferromagnetism in two-dimensional Pt dichalcogenides, Phys. Rev. B 94 (2016) 104426, https://doi.org/10.1103/PhysRevB.94.104426.

[20] L. Ao, H.Y. Xiao, X. Xiang, S. Li, K.Z. Liu, H. Huang, X.T. Zu, Functionalization of a GaSe

monolayer by vacancy and chemical element doping, Phys. Chem. Chem. Phys. 17 (2015) 10737-10748, https://doi.org/10.1039/c5cp00397k.

[21] S. Radhakrishnan, D. Das, A. Samanta, C.A. de los Reyes, L.Z. Deng, L.B. Alemany, T.K. Weldeghiorghis, V.N. Khabashesku, V. Kochat, Z.H. Jin, P.M. Sudeep, A.A. Marti, C.W. Chu, A. Roy, C.S. Tiwary, A.K. Singh, P.M. Ajayan, Fluorinated h-BN as a magnetic semiconductor, Sci. Adv. 3 (2017) e1700842, https://doi.org/10.1126/sciadv.1700842.

[22] H. Peng, H.J. Xiang, S.H. Wei, S.S. Li, J.B. Xia, J. Li, Origin and enhancement of hole-induced ferromagnetism in first-row d^0 semiconductors, Phys. Rev. Lett. 102 (2009) 017201, https://doi.org/10.1103/PhysRevLett.102.017201.

[23] T. Cao, Z. Li, S.G. Louie, Tunable magnetism and half-metallicity in hole-doped monolayer GaSe, Phys. Rev. Lett. 114 (2015) 236602, https://doi.org/10.1103/PhysRevLett.114.236602.

[24] N. Miao, B. Xu, N.C. Bristowe, J. Zhou, Z. Sun, Tunable magnetism and extraordinary sunlight absorbance in Indium triphosphide monolayer, J. Am. Chem. Soc. 139 (2017) 11125-11131, https://doi.org/10.1021/jacs.7b05133.

[25] Y.Q. Song, J.H. Yuan, L.H. Li, M. Xu, J.F. Wang, K.H. Xue, X.S. Miao, KTlO: a metal shrouded 2D semiconductor with high carrier mobility and tunable magnetism, Nanoscale 11 (2019) 1131-1139, https://doi.org/10.1039/c8nr08046a.

[26] S. Yu, J. Tang, Y. Wang, F. Xu, X. Li, X. Wang, Recent advances in two-dimensional ferromagnetism: strain-, doping-, structural- and electric field-engineering toward spintronic applications, Sci. Technol. Adv. Mater. 23 (2022) 140-160, https://doi.org/10.1080/14686996.2022.2030652.

[27] L. Seixas, A.S. Rodin, A. Carvalho, A.H. Castro Neto, Multiferroic two-dimensional materials, Phys. Rev. Lett. 116 (2016) 206803, https://doi.org/10.1103/PhysRevLett.116.206803.

[28] D.K. Efetov, P. Kim, Controlling electron-phonon interactions in graphene at ultrahigh carrier densities, Phys. Rev. Lett. 105 (2010) 256805, https://doi.org/10.1103/PhysRevLett.105.256805.

[29] J.T. Ye, S. Inoue, K. Kobayashi, Y. Kasahara, H.T. Yuan, H. Shimotani, Y. Iwasa, Liquid-gated interface superconductivity on an atomically flat film, Nat. Mater. 9 (2010) 125-128, https://doi.org/10.1038/nmat2587.

[30] Y.J. Zhang, T. Oka, R. Suzuki, J.T. Ye, Y. Iwasa, Electrically switchable chiral light-emitting transistor, Science 344 (2014) 725-728, https://doi.org/10.1126/science.1251329.

[31] S. Haastrup, M. Strange, M. Pandey, T. Deilmann, P.S. Schmidt, N.F. Hinsche, M.N. Gjerding, D. Torelli, P.M. Larsen, A.C. Riis-Jensen, J. Gath, K.W. Jacobsen, J. Jørgen Mortensen, T. Olsen, K.S. Thygesen, The Computational 2D Materials Database: high-throughput modeling and discovery of atomically thin crystals, 2D Mater. 5 (2018) 042002, https://doi.org/10.1088/2053-1583/aacfc1.

[32] M.N. Gjerding, A. Taghizadeh, A. Rasmussen, S. Ali, F. Bertoldo, T. Deilmann, N.R. Knøsgaard, M. Kruse, A.H. Larsen, S. Manti, T.G. Pedersen, U. Petralanda, T. Skovhus, M.K. Svendsen, J.J. Mortensen, T. Olsen, K.S. Thygesen, Recent progress of the Computational 2D Materials Database (C2DB), 2D Mater. 8 (2021) 044002, https://doi.org/10.1088/2053-1583/ac1059.

[33] D. Torelli, K.S. Thygesen, T. Olsen, High throughput computational screening for 2D ferromagnetic materials: the critical role of anisotropy and local correlations, 2D Mater. 6 (2019) 045018, https://doi.org/10.1088/2053-1583/ab2c43.

[34] N. Mounet, M. Gibertini, P. Schwaller, D. Campi, A. Merkys, A. Marrazzo, T. Sohier, I.E. Castelli, A. Cepellotti, G. Pizzi, N. Marzari, Two-dimensional materials from high-throughput computational exfoliation of experimentally known compounds, Nat. Nanotechnol. 13 (2018) 246-252, https://doi.org/10.1038/s41565-017-0035-5.

[35] D. Torelli, H. Moustafa, K.W. Jacobsen, T. Olsen, High-throughput computational screening for two-dimensional magnetic materials based on experimental databases of three-dimensional compounds, Npj Comput. Mater. 6 (2020) 158, https://doi.org/10.1038/s41524-020-00428-x.
[36] R. Meng, L. da Costa Pereira, J.-P. Locquet, V. Afanas'ev, G. Pourtois, M. Houssa, Hole-doping induced ferromagnetism in 2D materials, Npj Comput. Mater. 8 (2022) 230, https://doi.org/10.1038/s41524-022-00916-2.
[37] J. Nelson, S. Sanvito, Predicting the Curie temperature of ferromagnets using machine learning, Phys. Rev. Mater. 3 (2019) 104405, https://doi.org/10.1103/PhysRevMaterials.3.104405.
[38] S.M. Lundberg, G. Erion, H. Chen, A. DeGrave, J.M. Prutkin, B. Nair, R. Katz, J. Himmelfarb, N. Bansal, S.I. Lee, From local explanations to global understanding with explainable AI for trees, Nat. Mach. Intell. 2 (2020) 56-67, https://doi.org/10.1038/s42256-019-0138-9.
[39] R.H. Ouyang, S. Curtarolo, E. Ahmetcik, M. Scheffler, L.M. Ghiringhelli, SISSO: a compressed-sensing method for identifying the best low-dimensional descriptor in an immensity of offered candidates, Phys. Rev. Mater. 2 (2018) 083802, https://doi.org/10.1103/PhysRevMaterials.2.083802.
[40] R. Ouyang, E. Ahmetcik, C. Carbogno, M. Scheffler, L.M. Ghiringhelli, Simultaneous learning of several materials properties from incomplete databases with multi-task SISSO, J. Phys. Mater. 2 (2019) 024002, https://doi.org/10.1088/2515-7639/ab077b.
[41] C.M. Acosta, E. Ogoshi, J.A. Souza, G.M. Dalpian, Machine learning study of the magnetic ordering in 2D materials, ACS Appl. Mater. Interfaces 14 (2022) 9418-9432, https://doi.org/10.1021/acsami.1c21558.
[42] P.E. Blochl, Projector augmented-wave method, Phys. Rev. B Condens. 50 (1994) 17953-17979, https://doi.org/10.1103/PhysRevB.50.17953.
[43] G. Kresse, J. Furthmuller, Efficient iterative schemes for ab initio total-energy calculations using a plane-wave basis set, Phys. Rev. B Condens. 54 (1996) 11169-11186, https://doi.org/10.1103/PhysRevB.54.11169.
[44] J.P. Perdew, K. Burke, M. Ernzerhof, Generalized gradient approximation made simple, Phys. Rev. Lett. 77 (1996) 3865-3868, https://doi.org/10.1103/PhysRevLett.77.3865.
[45] S. Grimme, J. Antony, S. Ehrlich, H. Krieg, A consistent and accurate ab initio parametrization of density functional dispersion correction (DFT-D) for the 94 elements H-Pu, J. Chem. Phys. 132 (2010) 154104, https://doi.org/10.1063/1.3382344.
[46] H.J. Monkhorst, J.D. Pack, Special points for Brillouin-zone integrations, Phys. Rev. B 13 (1976) 5188-5192, https://doi.org/10.1103/PhysRevB.13.5188.
[47] Y.W. Son, M.L. Cohen, S.G. Louie, Half-metallic graphene nanoribbons, Nature 444 (2006) 347-349, https://doi.org/10.1038/nature05180.
[48] N.C. Bristowe, M. Stengel, P.B. Littlewood, E. Artacho, J.M. Pruneda, One-dimensional half-metallic interfaces of two-dimensional honeycomb insulators, Phys. Rev. B 88 (2013) 161411, https://doi.org/10.1103/PhysRevB.88.161411.
[49] K. Sheng, H.-K. Yuan, Z.-Y. Wang, Intrinsic ferromagnetism in 2D h-CrC semiconductors with strong magnetic anisotropy and high Curie temperatures, J. Mater. Chem. C, 9 (2021) 16495-16505, https://doi.org/10.1039/d1tc04389g.
[50] Y. Sun, Z. Zhuo, X. Wu, Bipolar magnetism in a two-dimensional NbS_2 semiconductor with high Curie temperature, J. Mater. Chem. C 6 (2018) 11401-11406, https://doi.org/10.1039/c8tc04188a.
[51] A. Hjorth Larsen, J. Jorgen Mortensen, J. Blomqvist, I.E. Castelli, R. Christensen, M. Dulak, J. Friis, M.N. Groves, B. Hammer, C. Hargus, E.D. Hermes, P.C. Jennings, P. Bjerre Jensen, J. Kermode, J.R.

Kitchin, E. Leonhard Kolsbjerg, J. Kubal, K. Kaasbjerg, S. Lysgaard, J. Bergmann Maronsson, T. Maxson, T. Olsen, L. Pastewka, A. Peterson, C. Rostgaard, J. Schiotz, O. Schutt, M. Strange, K.S. Thygesen, T. Vegge, L. Vilhelmsen, M. Walter, Z. Zeng, K.W. Jacobsen, The atomic simulation environment-a Python library for working with atoms, J. Phys. Condens. Matter. 29 (2017) 273002, https://doi.org/10.1088/1361-648X/aa680e.

[52] E.C. Stoner, Collective electron ferromagnetism II. Energy and specific heat, Proc. Math. Phys. Eng. Sci. 169 (1939) 339-371, https://doi.org/10.1098/rspa.1939.0003.

[53] T. Xie, J.C. Grossman, Crystal graph convolutional neural networks for an accurate and interpretable prediction of material properties, Phys. Rev. Lett. 120 (2018) 145301, https://doi.org/10.1103/PhysRevLett.120.145301.

[54] A. Dunn, Q. Wang, A. Ganose, D. Dopp, A. Jain, Benchmarking materials property prediction methods: the Matbench test set and Automatminer reference algorithm, Npj Comput. Mater. 6 (2020) 138, https://doi.org/10.1038/s41524-020-00406-3.

Dr. Junqiu An received his B.S. degree in Electronic Information Science and Technology from Southwest Jiaotong University, Chengdu, China in 2021. He is currently working toward the M.S. degree in Physics with the school of physical science and technology, Southwest Jiaotong University, Chengdu, China. His research interests include nanomaterials and materials informatics.

Dr. Jiao Chen received her B.S. degree in Materials Science and Engineering from Leshan Normal University, Leshan, China in 2018. She is currently working toward the Ph.D. degree in Physics with the school of physical science and technology, Southwest Jiaotong University, Chengdu, China. Her research interests include optoelectronic materials and catalysis.

Dr. Xiaotao Zhang received his B.S. degree in Applied Physics from Southwest Jiaotong University, Chengdu, China, in 2020. He is currently working toward the M.S. degree in Physics with the school of physical science and technology, Southwest Jiaotong University, Chengdu, China. His research interests include optoelectronic materials and machine learning.

Prof. Hongyan Wang received her Ph. D. degree in Fudan University in 1999. She is the ministry of education in the new century excellent talents scheme, the sichuan province outstanding youth leader funding scheme, the academic and technical leaders of sichuan province, and the outstanding contribution expert. Her research focused on nanoscaled materials.

Prof. Yongliang Tang received his Ph.D. in 2017 from the University of Electronic Science and Technology of China. He became an associate professor in 2018 in Southwest Jiaotong University. His research interests include studying nanomaterials for catalyst and sensor applications.

Yuxiang Ni received his PhD degree in Energy in the year of 2013 from Ecole Centrale Paris, France. He then worked in the University of Minnesota, Twin cities (2014-1016) as a postdoc research associate. He is now a professor in the School of Physical Science and Technology in Southwest Jiaotong University. His research focus on nanoscale heat transfer and structural design of functional materials.

Prof. Yuan Ping Feng received his B.Sc. degree from Lanzhou University in 1982 and Ph.D. from Illinois Institute of Technology in 1987. He is currently a Professor in the Department of Physics, and Head of Theory Group at the Centre for Advanced 2D Materials, NUS. His research interest is in computational materials physics.

Dr. Lei Shen graduated from the Department of Physics at the National University of Singapore (NUS), Singapore. He is currently a Senior Lecturer in Mechanical Engineering at NUS. His research interests include computational physics and materials informatics.

Dr. Haiyan Lu graduated from the Institute of Theoretical Physics, Chinese Academy of Sciences. She is the associate professor and doctoral supervisor of Institute of Materials, China Academy of Engineering Physics. She devotes to the research on the strongly correlated electronic systems and functional material design, especially for lanthanide and actinide magnetic systems.

Prof. Yuanzheng Chen received his Ph.D. degree in State Key Lab of Superhard Materials of Jilin University in 2014. He is currently a professor and doctoral supervisor of school of physical science and technology, Southwest Jiaotong University. His research interest is in computational materials physics and nano energy materials.